Formation of Giant Unilamellar Vesicles from Spin-Coated Lipid Films by Thermal Radiation

Céline Billerit, Gavin D. M. Jeffries, Owe Orwar, and Aldo Jesorka

Electronic Supplementary Information (ESI)

Table of contents

Materials and Methods

Lipids

Soybean polar lipid extract (SPE), l-stearoyl-2-arachidonoyl-*sn*-glycero-3-phosphoethanolamine (PE), 1-palmitoyl-2-oleoyl-*sn*-glycero-3-phosphocholine (POPC), 1,2-dimyristoyl-*sn*-glycero-3-phosphocholine (DMPC), 1,2-dioleoyl-*sn*-glycero-3-phospho-L-serine (DOPS), 1,2-dioleoyl-3-trimethylammonium-propane (DOTAP) were purchased from Avanti Polar Lipids and Texas Red 1,2-dihexadecanoyl-*sn*-glycero-3-phosphoethanolamine (Texas Red DHPE) was purchased from Sigma-Aldrich. All lipids were dissolved in chloroform (Sigma-Aldrich) prior to solution preparation.

Surface fabrication

Borosilicate cover slips (#1, VWR) were thoroughly cleaned and plasma treated using microwave generated oxygen plasma (TePla 300 PC, PVA TePla AG), at a power of 250 W for 2 minutes. SiO_2 was deposited onto the cleaned cover slips by reactive sputtering, using a sputter system (MS 150, FHR), to a final film thickness of 84 nm. The surfaces were used immediately after fabrication.

Lipid film preparation

Lipid thin films were prepared on SiO_2 surfaces by using the spin-coated method detailed by Estes and Mayer.[1] Briefly, we deposited 0.7 mL of 0.7 mg/mL lipids dissolved in chloroform on SiO_2 surface and allowed 2-5 seconds to fully spread over the entire surface. Using an in-house spin-coater, the lipid-spread cover slip was subsequently spun at a speed of 600 rpm for 10 minutes until the lipid film became dry. After formation of the lipid films, they were dried under vacuum for 2 hours in a dessicator to remove all the remaining traces of solvent.

Lipid spin-coated surfaces storage

After drying, the lipid spin-coated surfaces were transferred to a plastic box for protective storage. This box was stored at room temperature in a sealed anti-static plastic bag, containing a desiccant to control humidity.

Heating system

The vesicle system was heated using direct introduction of IR-B radiation through an optical fiber. A 1470 nm semiconductor diode laser (HHF-1470-6-95, Seminex) driven with an 8 A power source (4308 Laser Source, Arroyo Instruments) was used in combination with a 50 µm core diameter, 0.22 NA multimode optical fiber (Ocean Optics). The fiber was prepared by removing the outer sheath cladding, followed by carefully cutting and polishing using a fiber cleaning kit (Ocean Optics). The heating system was calibrated using a temperature-dependent fluorescent dye Rhodamine B with the aid of a microfluidic device.[2,3] The fiber output was located around at 40-50 µm from the surface, at which the vesicles form, resulting in a volume of approximately 1 nL being efficiently heated.

Experimental setup

A rectangular frame created from poly(dimethylsiloxane) (PDMS) was positioned onto the lipid coated surface, defining a chamber. This chamber is filled with 2 mL of a buffer solution prior to experimentation. Two phosphate buffered saline (PBS) solutions with different ionic strength were used to hydrate the lipids films: (i) 60 mM ionic strength PBS solution containing 5 mM Trizma base, 30 mM

K_3PO_4, 30 mM KH_2PO_4 and 0.5 mM NaEDTA, pH 7.8. (ii) 140 mM ionic strength PBS solution containing 2.7 mM KCl and 137 mM NaCl, pH 7.4.

Immediately after lipid film hydration, we locally heated the lipid film at approximately 90°C by applying direct laser radiation. Liposomes formed within a few seconds, but we allowed the heating to continue for at least 5 minutes, until the liposomes grew to a sufficiently large size. It should be noted that the heat-induced formation of vesicles was not possible at all locations on the spin-coated surface. It was visually apparent that the lipid distribution was not wholly even, possibly due to insufficient spin-speed used or in-homogenously distributed lipid within the solution. The result of which led to a variances of thickness at different location in the film. Locations, at which the lipid film appeared thin, were difficult to drive vesicle formation, indicating that the mechanism depends also on the thickness of the lipid film.

To generate a greater number of vesicles, the whole hydrated lipid film was heated for 30 minutes at 80°C in a laboratory oven (Venticell, MMM). The resulting vesicles were harvested from the chamber using a plastic pipette and introduced into a separate PBS solution.

Encapsulation

Dextran (average mol. wt 3,000-5,000) labeled with fluorescein isothiocyanate (FITC), fluorescein sodium salt and dextran (mol. wt 5,000) were purchased from Sigma-Aldrich. In one instance FITC-dextran was encapsulated inside forming/formed vesicles by adding it to the PBS solution either before or just after heat-induced vesicle formation. Fluorescein encapsulation was also achieved inside forming vesicles, by adding separately fluorescein and dextran to the PBS solution before heat-induced vesicle formation. The final concentrations of FITC-dextran, fluorescein and dextran in the PBS solution were 0.02 mg/mL.

Imaging

A confocal laser scanning microscopy system (Leica TCS SP2 RS), with a HCX PL APO CS 40x/1.25 oil immersion objective, was used for the acquisition of micrographs. The differential interference contrast (DIC) mode was applied and bright field images were captured using either a Prosilica GX1920 high resolution camera (Allied Vision Technologies) or Chameleon CMLN-1352M USB 2.0 digital camera (Point Grey) with in-house programmed acquisition software using Labview 2009 (National Instruments). Texas Red DHPE and fluorescein were excited at 594 nm using a He/Ne laser and 488 nm using an Ar^+/ArKr laser respectively. The emitted light was collected by a photomultiplier tube using the AOBS module, within the ranges 600-700 nm for Texas Red DHPE and 500-600 nm for fluorescein.

Encapsulation efficiency

We determined the encapsulation efficiency within individual GUVs by quantification of the fluorescence intensity inside forming vesicles. The encapsulation of FITC-dextran inside vesicles was compared to the encapsulation of fluorescein unconjugated to dextran. In total 200 hundred vesicles were analyzed; 100 vesicles for the FITC-dextran encapsulation and 100 vesicles for the fluorescein encapsulation. The size of the vesicles ranged from 5-30 µm, where the vesicle membranes were visualized by incorporating 1% of Texas Red DHPE.

Fluorescence from fluorescein could be seen both inside and outside vesicles, however utilizing a confocal arrangement with a pinhole set to 0.25 Airy, the fluorescent contribution from the solution (more than 2 µm either side of the focal plane) was effectively removed. Images were formed using laser scanning confocal microscopy, while maintaining the fluorescent excitation intensity and the confocal acquisition settings.

A typical example of this fluorescence measurement is shown in Figure S6A, where the dashed line denotes a ROI inside a vesicle and the solid line denotes the ROI of the external solution. It should be noted that although the ROIs are drawn and displayed on the image displaying the vesicle membranes (red channel), the data extracted for analysis was from the green fluorescein image (green channel). Through intensity analysis, and subsequent subtraction of the background directly surrounding the vesicle, an accurate value for the fluorescence intensity inside each vesicle could be measured. The encapsulation efficiency within individual vesicles was quantified by the ratio of the fluorescence intensity inside each vesicle to that in the external solution (Fig. S7). Encapsulation efficiencies were measured as 0.79 ± 0.18 and 0.77 ± 0.10 for FITC-dextran and fluorescein unconjugated to dextran respectively.

Lamellarity

We investigated the vesicle properties, through analysis of the lamellarity, utilising fluorescence measurement of the membrane. The fluorescence intensity of vesicles generated by thermal radiation was compared to those formed by the commonly used technique, dehydration-rehydration.

In total 50 vesicles were analyzed; 25 obtained by thermal radiation and 25 obtained by dehydration-rehydration, the membranes of which were visualised by incorporating 1% of Texas Red DHPE. Images were formed using laser scanning confocal microscopy, while maintaining the fluorescent excitation intensity and the confocal acquisition settings, for all the vesicles under observation.

A typical example of this fluorescence measurement is shown in Figure S8, where the dashed lines denote the region of interest (ROI). To obtain a representative sample, this ROI was selected at a distance away from any interference (such the fluorescence blooming from the multilamellar vesicle connected to the unilamellar vesicle, or the influence of a connected interface), while maintaining a minimum membrane inclusion of 50%. Through intensity analysis, and subsequent subtraction of the background directly surrounding the vesicle, an accurate value for the membrane intensity could be measured. Using the analysis scheme proposed by Akashi et al,[4] we propose that a distribution of lamellarities was present. Assuming that the population measured was sufficiently large to capture unilamellar vesicles, ROI intensity measurements will indicate any occurring distribution. The lowest intensity grouping of which should therefore be representative of a unilamellar membrane. This value was utilized as a normalization factor, to estimate the lamellarity for each vesicle, mirroring the technique proposed by Akashi et al. The measured distribution was found to be almost identical for vesicles formed by both thermal radiation and by dehydration-rehydration (Figure S9). These results indicate that generation by the thermal radiation technique does not significantly influence the distribution of lamellarity.

Vesicle preparation by dehydration-rehydration method

A suspension of small unilamellar vesicles generated from 99% SPE and 1% Texas Red DHPE (6 mg/mL) was prepared. This was further processed using the dehydration-rehydration method described by Criado and Keller,[5] with modifications[6] for the preparation of GUVs. For the dehydration step, a 7 mL droplet of this suspension was placed onto a borosilicate cover slip and dehydrated in a vacuum dessicator for 10 minutes. When the lipid film was dry, it was rehydrated using 60 mM ionic strength PBS solution. After the vesicles were formed, they were carefully transferred to the PDMS chamber, filled with 2 mL of PBS solution.

Supporting figures

Fig. S1 – Monitoring vesicle stability

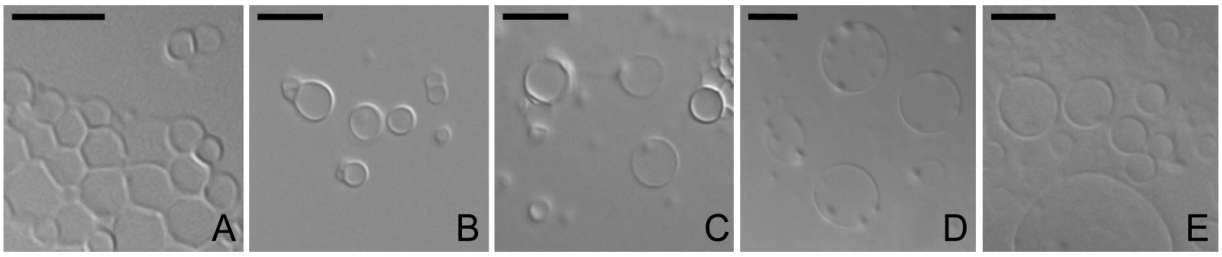

Figure S1. DIC images of vesicles recorded 30 minutes after formation, formed from different types of lipids. (A-E) display vesicles formed from POPC, DOPS, DMPC, PE, SPE respectively. The scale bars represent 10 µm. All images were recorded using a 40x/1.25 NA objective and a high-resolution camera.

Fig. S2 – GUVs formed from DOTAP lipid film

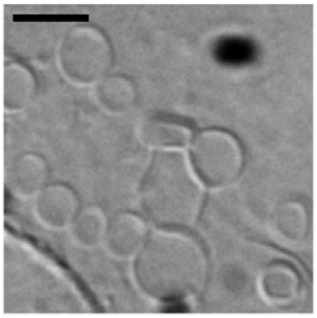

Figure S2. A DIC image of GUVs generated from a DOTAP lipid film, hydrated with 140 mM ionic strength PBS solution. At 60 mM ionic strength, only few small vesicles were observed. This variance can be explained by the possible attraction between the SiO_2 surface, exhibiting a native negative charge, and the DOTAP lipid film, which is positively charged. The scale bar represents 5 µm. The image was recorded using a 40x/1.25 NA objective and a Chameleon digital camera.

Fig. S3 – Progressive growth sequence

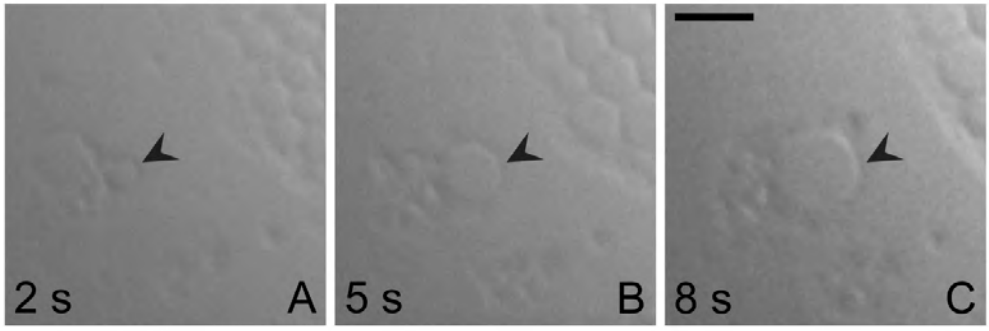

Figure S3. Process of heat-induced formation of a vesicle. DIC images of a vesicle from POPC lipid film, growing during the heating. (A-C) display a progressive growth sequence after 2, 5 and 8 seconds of heating. The arrow indicated the vesicle under observation. The scale bar represents 5 µm. All images were recorded using a 40x/1.25 NA objective and a high-resolution camera.

Fig. S4 – A 3D reconstruction of formed vesicles during the heating process

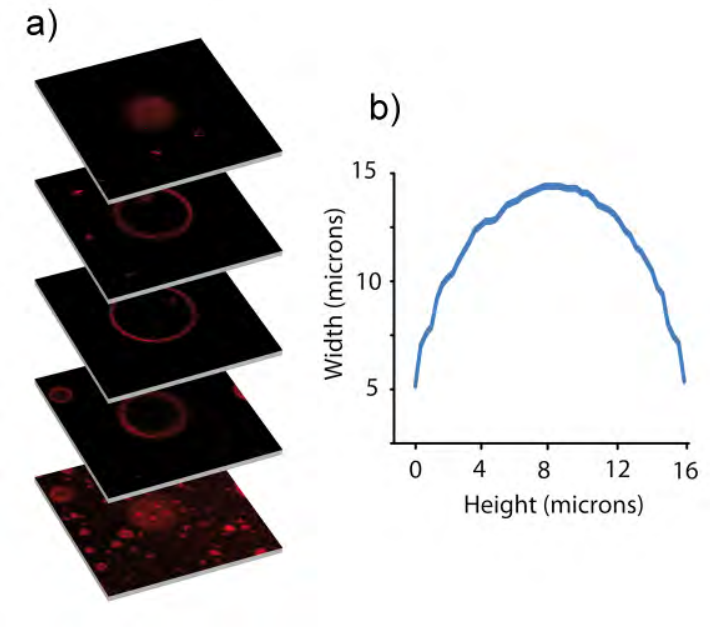

Figure S4. 3D analysis of a typical vesicle after formation. (A) displays extracted planes from an XYZ stack performed using confocal microscopy. It clearly shows the vesicle has a volume isolated from the surface, with an almost spherical geometry. (B) is a vesicle width plot measured at each confocal sectioning plane. The extracted data confirms the almost spherical shape. The slight elongation of the vesicle is likely due to motion of the vesicle during imaging.

Fig. S5 – GUVs formed at high ionic strength

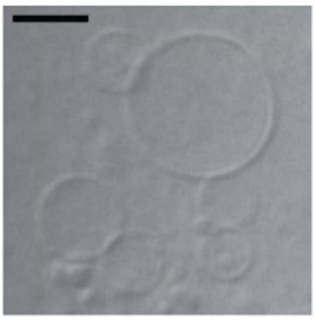

Figure S5. A DIC image of GUVs generated from an SPE lipid film hydrated with 140 mM ionic strength PBS solution. The scale bar represents 5 µm. The image was recorded using a 40x/1.25 NA objective and a Chameleon digital camera.

Fig. S6 – Encapsulation of fluorescein into GUVs by means of dextran

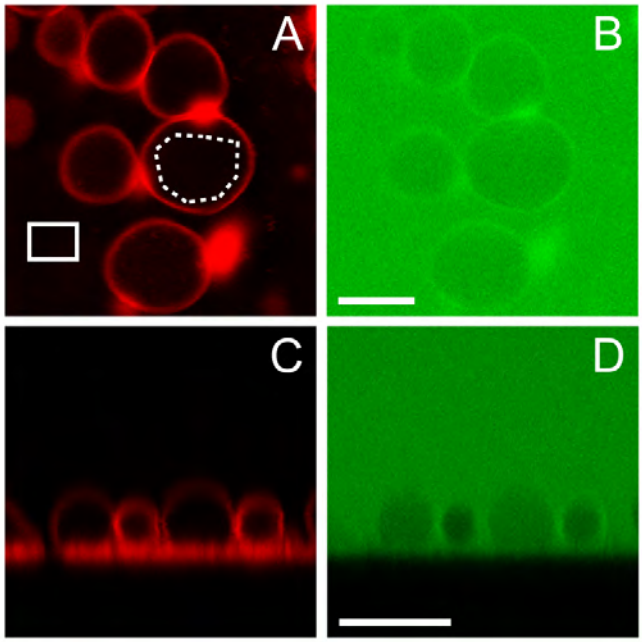

Figure S6. Confocal laser scanning micrographs of forming vesicles from 99% SPE and 1% Texas Red DHPE, during encapsulation of fluorescein. (A-D) display encapsulation variances during the formation procedure. Separate XY confocal laser scanning micrographs for the red (Texas Red DHPE) and green (fluorescein) channels are shown in A and B respectively. Dashed line area represents the ROI inside the vesicle measurement and the solid line area the ROI of the external solution. The scale bar in (B) represents 10 µm, valid for (A). Separate XZ confocal laser scanning micrographs for the red (Texas Red DHPE) and green (fluorescein) channels are shown in C and D respectively. The scale bar in (D) represents 10 µm, valid for (C). The pinhole was reduced to 0.25 airy to minimize contributions from out of focus fluorescence in the solution. Variances in fluorescence intensity within the vesicles therefore represent the variances of encapsulation.

Fig. S7 – Encapsulation Efficiency

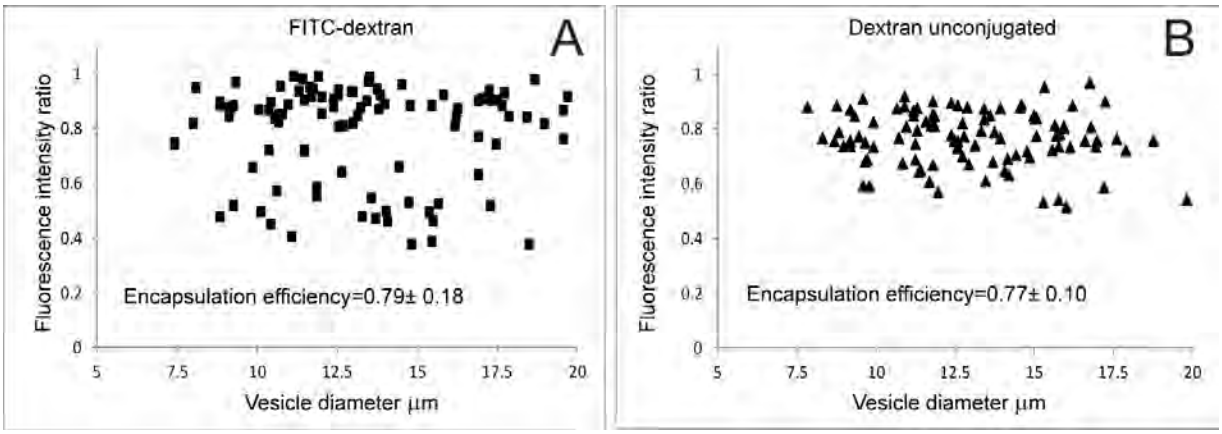

Figure S7. Encapsulation efficiencies for both FITC-dextran and fluorescein unconjugated to dextran. Fluorescence intensity ratios were performed for each individual vesicle. (A) Encapsulation efficiency of FITC-dextran. (B) Encapsulation efficiency of fluorescein unconjugated to dextran. Encapsulation efficiencies were measured as 0.79 ± 0.18 and 0.77 ± 0.10 for FITC-dextran and fluorescein unconjugated to dextran respectively.

Fig. S8 – Fluorescence measurement examples

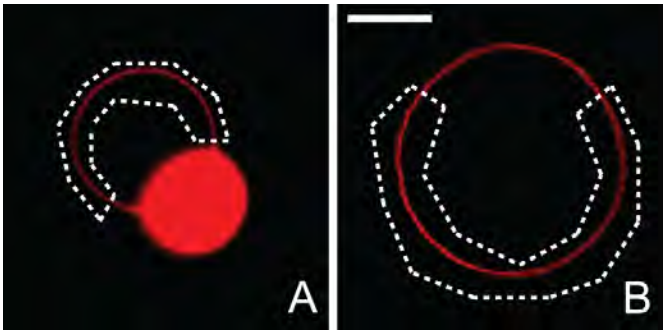

Figure S8. Confocal laser scanning micrographs of GUVs from 99% SPE and 1% Texas Red DHPE. Dashed lines areas represent the ROI chosen for the fluorescence measurement. (A) Example of one GUV obtained by dehydration-rehydration method. (B) Example of one GUV obtained by thermal radiation. The scale bar represents 10 µm, valid for (A).

Fig. S9 – Lamellarity estimation

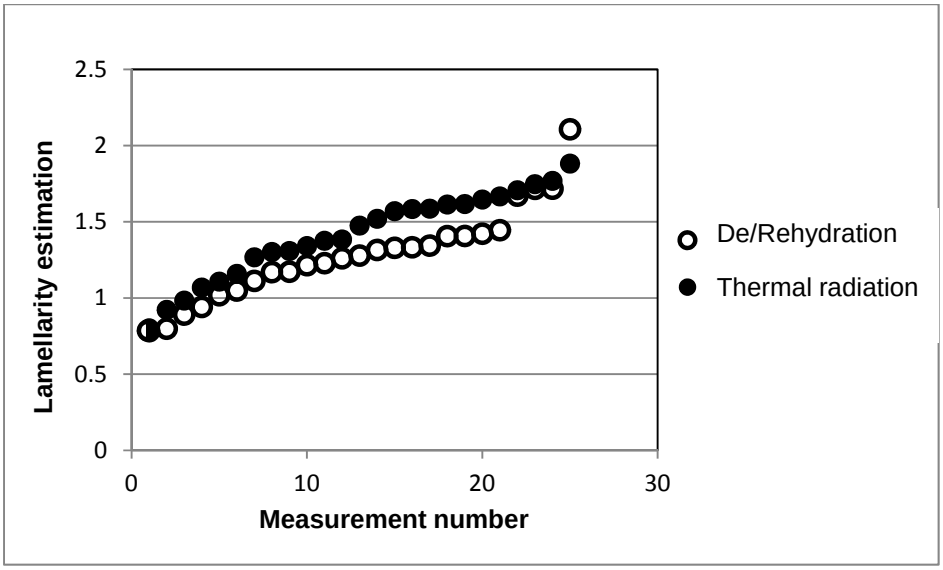

Figure S9. Distribution of lamellarity estimate of liposomes, generated using both thermal radiation and dehydration-rehydration techniques.

Fig. S10 – Lipid film storage tests

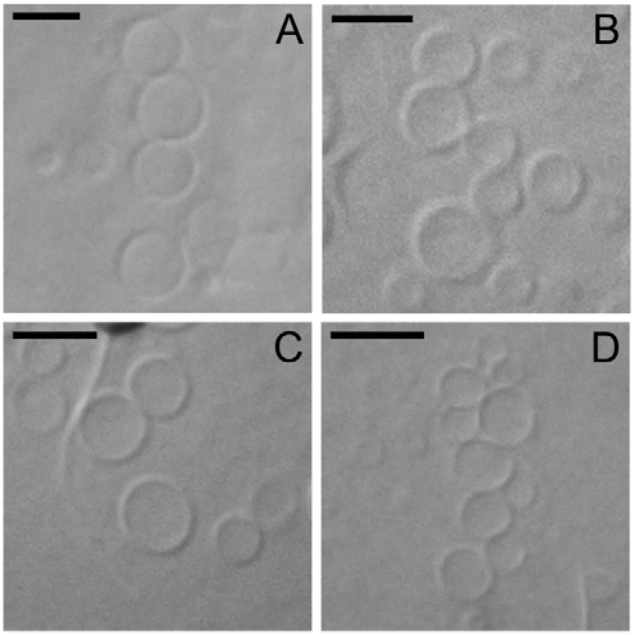

Figure S10. DIC images of SPE GUVs, formed from spin-coated lipid surfaces, which had been dry stored for various times. (A-D) display the storage times 1, 3, 7 and 30 days respectively. No apparent variances could be seen in either the size or distribution of the formed vesicles after any of the storage periods. The scale bars represent 5 µm. All images were recorded using a 40x/1.25 NA objective and a Chameleon digital camera.

References

[1] D. J. Estes, M. Mayer, *Colloids and surfaces. B, Biointerfaces* **2005**, *42*, 115-23.

[2] D. Ross, M. Gaitan, L. E. Locascio, *Analytical chemistry* **2001**, *73*, 4117-23.

[3] A. Ainla, E. T. Jansson, N. Stepanyants, O. Orwar, A. Jesorka, *Analytical chemistry* **2010**, *82*, 4529-36.

[4] K. Akashi, H. Miyata, H. Itoh, K. Kinosita, *Biophysical journal* **1996**, *71*, 3242-50.

[5] M. Criado, B. U. Keller, *FEBS letters* **1987**, *224*, 172-6.

[6] M. Karlsson, K. Nolkrantz, M. J. Davidson, A. Strömberg, F. Ryttsén, B. Akerman, O. Orwar, *Analytical chemistry* **2000**, *72*, 5857-62.